

A three-state model with loop entropy for the over-stretching transition of DNA

Thomas R. Einert,^{1,*} Douglas B. Staple,^{2,3} Hans-Jürgen Kreuzer,² and Roland R. Netz^{1,†}

¹*Physik Department, Technische Universität München, 85748 Garching, Germany*

²*Department of Physics and Atmospheric Science, Dalhousie University, Halifax, B3H 3J5 Canada*

³*Max-Planck-Institut für Physik komplexer Systeme, 01187 Dresden, Germany*

(Dated: November 10, 2018)

We introduce a three-state model for a single DNA chain under tension that distinguishes between B-DNA, S-DNA, and M (molten or denatured) segments and at the same time correctly accounts for the entropy of molten loops, characterized by the exponent c in the asymptotic expression $S \sim -c \ln n$ for the entropy of a loop of length n . Force extension curves are derived exactly employing a generalized Poland-Scheraga approach and compared to experimental data. Simultaneous fitting to force-extension data at room temperature and to the denaturation phase transition at zero force is possible and allows to establish a global phase diagram in the force-temperature plane. Under a stretching force, the effects of the stacking energy, entering as a domain-wall energy between paired and unpaired bases, and the loop entropy are separated. Therefore we can estimate the loop exponent c independently from the precise value of the stacking energy. The fitted value for c is small, suggesting that nicks dominate the experimental force extension traces of natural DNA.

I. INTRODUCTION

DNA continuously stays in focus of polymer scientists due to its unique mechanical and structural properties. In particular the possibility to trigger phase transformations in this one-dimensional system has intrigued theorists from different areas [1]. In fact, the thermal denaturation or melting transition of DNA was shown to correspond to a true phase transition, brought about by a logarithmic contribution to the configurational entropy of molten loops or bubbles, $S \sim -c \ln n$, as a function of the loop size n [2]. The value of the exponent c is crucial since it determines the resulting transition characteristics. For $c = 3/2$, the value for a phantom chain without self-avoidance, the transition is continuous, while self-avoidance increases c slightly beyond the threshold $c = 2$ above which the transition becomes discontinuous [2, 3]. A distinct mechanism for transforming DNA involves the application of an extensional force. For forces around $F \approx 65$ pN DNA displays a highly cooperative transition and its contour length increases by a factor of roughly 1.7 to 2.1 over a narrow force range [4–6]. These experiments sparked a still ongoing debate on whether this over-stretching transition produces a distinct DNA state, named S-DNA, or merely the denatured state under external tension. According to the first view S-DNA is a highly stretched state with paired bases but disrupted base stacking [7–13]. In the other view the over-stretched state consists of two non-interacting strands [14–17]. Evidence for the existence of a distinct S-state comes from theoretical models [7, 9], molecular dynamics simulations [10–13] and from AFM experiments of Rief et al. [18–20] where in addition to the over-stretching transition a second weak transition at forces between 150 pN and 300 pN is discerned, which has been interpreted as a force induced melting of the S-state. The critical force of both transitions depends on the actual sequence [19] and the salt concentration [21], but the interpretation of the second transition is complicated by the occurrence of pronounced hysteresis effects that depend on various parameters such as pulling velocity, salt concentration, or presence of co-solutes such as cisplatin [19, 20]. On the other hand, support for the view according to which S-DNA is not a distinct state comes from theoretical models [14, 15], simulations [22] and recent experiments by Shokri et al. [16] and van Mameren et al. [17].

Apart from simulations [10–13], existing theoretical works that grapple with experimental force traces or DNA melting fall into three categories with increasing computational complexity, for reviews see refs. [23–25]. In the first group are Ising-like models for DNA under tension which give excellent fitting of the over-stretching transition but by construction cannot yield the denaturing transition [15, 26–28]. The work of Marko [29] is similar but employs a continuous axial strain variable. In the second group are models that include a logarithmic entropy contribution of molten loops in the spirit of the classical model by Poland and Scheraga [2] [3, 9, 30–34]. This gives rise to effectively long-ranged interactions between base pairs and thus to a true phase transition. The third group consists of models which explicitly consider two strands [35–39]. Those models thereby account for the configurational entropy of loops – at the cost of considerable calculational efforts – and correspond to loop exponents $c = d/2$ in the absence of

*Corresponding author: Physik Department, Technische Universität München, James-Franck-Straße, 85748 Garching, Germany, Tel.: +49-89-28914337

†E-mail: netz@ph.tum.de

self-avoidance effects, where the dimensionality of the model is $d = 3$ for ref. [35–37] and 1 for ref. [38, 39]. All these above mentioned works consider only two different base states (paired versus unpaired) and thus do not allow to distinguish between B-DNA, S-DNA and denatured bases. Recently, three-state models were introduced that yield very good fits of experimental force traces at ambient temperatures. However, in previous analytic treatments of such three-state models [7, 40], the loop entropy was neglected and therefore the temperature-induced denaturation in the absence of force cannot be properly obtained, while the loop entropy was included in a simulation study where most attention was given to dynamic effects [9].

In this paper we combine the Poland-Scheraga formalism with a three-state transfer matrix approach which enables us to include three distinct local base pairing states and at the same time to correctly account for long-ranged interactions due to the configurational entropy of molten DNA bubbles. Our approach thus allows for a consistent description of thermal denaturation and the force induced BS-transition within one framework and yields the global phase diagram in the force-temperature plane. We derive a closed form expression for the partition function of three-state DNA under tension. This allows to systematically investigate the full parameter range characterizing the three states and the DNA response to temperature and external force. In our model we allow for the existence of S-DNA but stress that the actual occurrence of S-DNA is governed by the model parameters. By assuming such a general point of view, our work is able to shed new light on the question of the existence of S-DNA. The extensible worm-like chain model is employed for the stretching response of each state. The loop exponent is found to have quite drastic effects on the force extension curve. For realistic parameters for the stacking energy, the experimental force extension curves are fitted best for small loop exponents $0 \leq c \leq 1$, hinting that the DNA in the experiments contained nicks. Loop exponents $c > 1$, which give rise to a genuine phase transition, are not compatible with experimental force-distance curves. Under external force, the effects of stacking energy and loop exponent are largely decoupled, since the stacking energy only determines the cooperativity of the BS-transition while the loop exponent influences the second SM-transition found at higher forces. This allows to disentangle these two parameters, in contrast to the denaturation transition at zero force where the effects of these two parameters are essentially convoluted. The precise value of c is important also from a practical point of view, as it impacts the kinetics of DNA melting [9, 41], which is omnipresent in biological and bio-technological processes.

II. THREE-STATE MODEL

Double-stranded DNA is modeled as a one-dimensional chain with bases or segments that can be in three different states, namely paired and in the native B-state, in the paired stretched S-state, or in the molten M-state. The free energy of a region of n segments in the same state reads

$$E_i(n, F) = n \cdot g_i(F) - \delta_{i,M} \cdot k_B T \ln n^{-c}, \quad (1)$$

with $i = B, S, M$. The force F dependent contribution

$$g_i(F) = g_i^0 + g_i^{\text{stretch}}(F) + g_i^{\text{WLC}}(F) \quad (2)$$

is split into three parts. g_i^0 is a constant that accounts for the base pairing as well as the difference of reference states of the worm-like stretching energy, *cf.* supporting material eq. (??). The stacking energy of neighboring bases in the same state is absorbed into g_i^0 , too, so that the stacking energy will appear explicitly only as an interfacial energy V_{ij} between two regions which are in a different state. The second term $g_i^{\text{stretch}} = -F^2 l_i / (2 \cdot \kappa_i)$ takes into account stretching along the contour with l_i and κ_i the segmental contour length and the elastic stretch modulus. Finally, $g_i^{\text{WLC}}(F)$ is the free energy of a worm-like chain (WLC) in the Gibbs ensemble (constant force F), based on the heuristic relation between force F and projected extension x [42] $F_i^{\text{WLC}}(x) \cdot \xi_i / k_B T = (1 - x/(nl_i))^{-2} / 4 + x/(nl_i) - 1/4$ where ξ_i is the persistence length and n the number of segments. The Gibbs free energy $n \cdot g_i^{\text{WLC}}(F)$ of a stretch of n segments is extensive in n and follows *via* integration, see supporting material section ???. We note that this is only valid if the persistence length is smaller than the contour length of a region, $\xi_i < nl_i$, which is a plausible assumption because of the high domain wall energies. Likewise, the decoupling of the free energy into contour stretching elasticity and worm-like chain elasticity is only approximate [43, 44] but quite accurate for our parameter values [45]: For small force WLC bending fluctuations dominate and the contour extensibility is negligible, while contour stretching sets in only when the WLC is almost completely straightened out. The last term in eq. (1) is the logarithmic configurational entropy of a molten loop ($i = M$), characterized by an exponent c [3, 30, 46], see supporting material section ???. The exponent is $c = 3/2$ for an ideal polymer [47] and 2.1 for a self avoiding loop with two attached helices [3, 48]. If the DNA loop contains a nick the exponent is reduced to $c = 0$ for an ideal polymer and 0.092 for a self avoiding polymer [3]. We consider the simple case $c = 0$, where transfer matrix methods can be used to yield results in the canonical ensemble with a fixed number of segments N [7], as well as the case of finite c where we introduce a modified Poland-Scheraga method to obtain results in the grand canonical ensemble.

III. PARTITION FUNCTION

A. Modified Poland-Scheraga approach for $c \neq 0$

The molecule is viewed as an alternating sequence of different regions each characterized by grand canonical partition functions. Various techniques for going back to the canonical ensemble are discussed below. The canonical partition function of a stretch of n segments all in state $i = B, S,$ or M is

$$\mathcal{Q}_i(n) = \exp(-\beta E_i(n)) , \quad (3)$$

where $\beta = (k_B T)^{-1}$ is the inverse thermal energy. The grand canonical partition functions are defined as $\mathcal{Z}_i = \sum_{n=1}^{\infty} \lambda^n \mathcal{Q}_i(n)$ with $\lambda = \exp(\beta\mu)$ the fugacity and μ the chemical potential. The grand canonical partition function of the whole DNA chain which contains an arbitrary number of consecutive B, S, and M stretches reads

$$\mathcal{Z} = \sum_{k=0}^{\infty} \mathbf{v}^T \cdot (\mathbf{M}_{\text{PS}} \mathbf{V}_{\text{PS}})^k \mathbf{M}_{\text{PS}} \cdot \mathbf{v} = \mathbf{v}^T \cdot (\mathbf{1} - \mathbf{M}_{\text{PS}} \mathbf{V}_{\text{PS}})^{-1} \mathbf{M}_{\text{PS}} \cdot \mathbf{v} , \quad (4)$$

with the matrices in this Poland-Scheraga approach given by

$$\mathbf{M}_{\text{PS}} = \begin{pmatrix} \mathcal{Z}_B & 0 & 0 \\ 0 & \mathcal{Z}_S & 0 \\ 0 & 0 & \mathcal{Z}_M \end{pmatrix} , \quad \mathbf{V}_{\text{PS}} = \begin{pmatrix} 0 & e^{-\beta V_{\text{BS}}} & e^{-\beta V_{\text{BM}}} \\ e^{-\beta V_{\text{SB}}} & 0 & e^{-\beta V_{\text{SM}}} \\ e^{-\beta V_{\text{MB}}} & e^{-\beta V_{\text{MS}}} & 0 \end{pmatrix} , \quad \mathbf{v} = \begin{pmatrix} 1 \\ 1 \\ 1 \end{pmatrix} \quad (5)$$

and where $\mathbf{1}$ is the unity matrix. The energies V_{ij} are the interfacial energies to have neighboring segments in different states and are dominated by unfavorable base pair un-stacking. The diagonal elements of \mathbf{V}_{PS} are zero which ensures that two neighboring regions are not of the same type and thus prevents double counting. The explicit form of \mathcal{Z} is given in the supporting material, see eq. (??). The partition function in eq. (4) is general and useful for testing arbitrary models for the three DNA states as given by the different \mathcal{Z}_i . This approach is also easily generalized to higher numbers of different states. Using the parameterization eq. (1) for vanishing loop exponent $c = 0$ the partition functions of the different regions are given by

$$\mathcal{Z}_i = \sum_{n=1}^{\infty} \lambda^n \mathcal{Q}_i(n) = \frac{\lambda e^{-\beta g_i}}{1 - \lambda e^{-\beta g_i}} , \quad \text{for } \lambda e^{-\beta g_i} < 1 , \quad (6)$$

$i = B, S, M$. Insertion into eq. (4) yields

$$\mathcal{Z}_{c=0} = \frac{a_1 \lambda + a_2 \lambda^2 + a_3 \lambda^3}{a_4 + a_5 \lambda + a_6 \lambda^2 + a_7 \lambda^3} . \quad (7)$$

which is a rational function of the fugacity λ , whose coefficients a_i – determined by eqs. (4) and (6) – are smooth functions of the force F and the temperature T . For $c \neq 0$ the partition function of a molten stretch is modified to

$$\begin{aligned} \mathcal{Z}_M &= \sum_{n=1}^{\infty} \lambda^n \mathcal{Q}_M(n) = \sum_{n=1}^{\infty} \lambda^n (e^{-\beta g_M})^n \frac{1}{n^c} \\ &= \text{Li}_c(\lambda e^{-\beta g_M}) , \quad \text{for } \lambda e^{-\beta g_M} < 1 \end{aligned} \quad (8)$$

where $\text{Li}_c(z) = \sum_{n=1}^{\infty} z^n n^{-c}$ for $z < 1$ is the polylogarithm [49] and exhibits a branch point at $z = 1$. The functional form of the grand canonical partition function for $c \neq 0$ reads

$$\mathcal{Z}_{c \neq 0} = \frac{b_0 \lambda + b_1 \lambda^2 + b_2 \text{Li}_c(\lambda/\lambda_b) + b_3 \lambda \text{Li}_c(\lambda/\lambda_b) + b_4 \lambda^2 \text{Li}_c(\lambda/\lambda_b)}{b_5 + b_6 \lambda + b_7 \lambda^2 + b_8 \lambda \text{Li}_c(\lambda/\lambda_b) + b_9 \lambda^2 \text{Li}_c(\lambda/\lambda_b)} , \quad (9)$$

where $\lambda_b = e^{\beta g_M}$ denotes the position of the branch point and the coefficients b_i , determined by eqs. (4), (6) and (8), are smooth functions of F and T .

The grand canonical ensemble where N , the total number of segments fluctuates, does not properly describe a DNA chain of fixed length. We therefore have to investigate the back-transformation into the canonical ensemble where the number of segments N is fixed. For the back-transformation there are three options:

1. *Calculus of residues route:*

The grand-canonical partition function $\mathcal{Z}(\lambda) = \sum_{N=1}^{\infty} \lambda^N \mathcal{Q}(N)$ can be viewed as a Laurent series, the coefficients of which are the canonical partition functions $\mathcal{Q}(N)$ determined exactly by

$$\mathcal{Q}(N) = \frac{1}{2\pi i} \oint_{\mathcal{C}} \frac{\mathcal{Z}(\lambda)}{\lambda^{N+1}} d\lambda. \quad (10)$$

The contour $\mathcal{C} = \lambda_0 e^{2\pi i t}$, $0 \leq t \leq 1$, is a circle in the complex plane around the origin with all singularities of $\mathcal{Z}(\lambda)$ lying outside. This complex contour integral can be evaluated using calculus of residues [50] which becomes technically involved for large N and thus limits the practical relevance of this route.

2. *Legendre transformation route:*

The canonical Gibbs free energy

$$\mathcal{G}(N) = -k_B T \ln \mathcal{Q}(N) \quad (11)$$

and the grand potential

$$\Phi(\mu) = -k_B T \ln \mathcal{Z}(\lambda), \quad (12)$$

are related *via* a Legendre transformation

$$\mathcal{G}(N) = \Phi(\mu(N)) + N \cdot \mu(N). \quad (13)$$

The chemical potential μ as a function of the segment number N is obtained by inverting the relation

$$N(\mu) = -\frac{\partial \Phi(\mu)}{\partial \mu}. \quad (14)$$

Let us briefly review the origin of eqs. (13) and (14) in the present context. Changing the integration variable in eq. (10) from λ to $\mu = \ln(\lambda)/\beta$, the complex path integral can be transformed into

$$\mathcal{Q}(N) = \int_{\mathcal{C}'} e^{-\beta \Phi(\mu) - \beta N \mu} d\mu \approx e^{-\beta \Phi(\mu_{\text{sp}}(N)) - \beta N \mu_{\text{sp}}(N)}, \quad (15)$$

with the contour $\mathcal{C}' = \mu_0 + 2\pi i t/\beta$, $0 \leq t \leq 1$ and $\mu_0 = k_B T \ln \lambda_0$. The integral in eq. (15) has been approximated by the method of steepest descent, where the contour \mathcal{C}' is deformed such that it passes through the saddle point μ_{sp} [50] determined by equation (14). If Φ features singularities deformation of the contour \mathcal{C}' requires extra care. In the present case the presence of a pole $\lambda_p = \exp(\beta \mu_p)$ of $\mathcal{Z}(\lambda)$ produces no problem as $\mu_{\text{sp}} < \mu_p$ holds, meaning that the deformed contour does not enclose the pole singularity. This is different for the branch point singularity μ_b where we will encounter the case $\mu_b < \mu_{\text{sp}}$ for large $c > 2$.

3. *Dominating singularity route:*

For large systems, *i. e.* $N \gg 1$, one approximately has $-\ln \mathcal{Q}(N) \sim N \ln \lambda_d$, where the dominant singularity $\lambda_d = \exp(\beta \mu_d)$ is the singularity (in the general case a pole or a branch point) of $\mathcal{Z}(\lambda)$ which has the smallest modulus. One thus finds

$$\mathcal{G}(N) = k_B T N \ln \lambda_d. \quad (16)$$

This easily follows from eq. (10): In the limit of $N \gg 1$ the integral can be approximated by expanding $\mathcal{Z}(\lambda)$ around λ_d and deforming \mathcal{C} to a Hankel contour which encircles λ_d [51]. For the case where $N(\mu) \propto (\mu_d - \mu)^{-\alpha}$, $\alpha > 0$, this can be understood also in the context of a Legendre transform. As $N = -\partial \Phi / \partial \mu$ one has $\Phi \propto (\mu_d - \mu)^{-\alpha+1}$ and therefore the first term of eq. (13) scales like $\Phi(\mu(N)) \propto N^{1-1/\alpha}$. Thus, the second term $N \mu(N) \propto N \mu_d - N^{1-1/\alpha} \propto N \mu_d$ is dominant. Since the saddle point behaves as $\mu_{\text{sp}} = \mu(N) \rightarrow \mu_d$ for $N \rightarrow \infty$, it follows that the dominating singularity expression eq. (16) equals the Legendre transform eq. (13) in the thermodynamic limit $N \rightarrow \infty$.

B. Transfer matrix approach for $c = 0$

For $c = 0$ only interactions between nearest neighbors are present and straight transfer matrix techniques are applicable. We introduce a spin variable i_n for each segment which can have the values $i_n = B, S, M$. The energetics are given by the Hamiltonian

$$H(i_1, i_2, \dots, i_N) = \sum_{n=1}^N g_{i_n} + \sum_{n=1}^{N-1} V_{i_n i_{n+1}} \quad (17)$$

where g_{i_n} and $V_{i_n i_{n+1}}$ are the previously introduced parameters for the segment and interfacial free energies. The canonical partition function of the molecule can be written as

$$\mathcal{Q}(N) = \sum_{i_1, \dots, i_N} e^{-\beta H(i_1, i_2, \dots, i_N)} = \mathbf{v}^T \cdot \mathbf{T}^{N-1} \mathbf{M}_{\text{TM}} \cdot \mathbf{v}, \quad (18)$$

where we introduced the transfer matrix $\mathbf{T} = \mathbf{M}_{\text{TM}} \mathbf{V}_{\text{TM}}$ and

$$\mathbf{M}_{\text{TM}} = \begin{pmatrix} e^{-\beta g_B} & 0 & 0 \\ 0 & e^{-\beta g_S} & 0 \\ 0 & 0 & e^{-\beta g_M} \end{pmatrix}, \quad \mathbf{V}_{\text{TM}} = \begin{pmatrix} 1 & e^{-\beta V_{BS}} & e^{-\beta V_{BM}} \\ e^{-\beta V_{SB}} & 1 & e^{-\beta V_{SM}} \\ e^{-\beta V_{MB}} & e^{-\beta V_{MS}} & 1 \end{pmatrix}, \quad \mathbf{v} = \begin{pmatrix} 1 \\ 1 \\ 1 \end{pmatrix}. \quad (19)$$

$\mathcal{Q}(N)$ is calculated readily by diagonalizing \mathbf{T}

$$\mathcal{Q}(N) = \mathbf{v}^T \cdot \mathbf{U} \mathbf{D}^{N-1} \mathbf{U}^{-1} \mathbf{M}_{\text{TM}} \cdot \mathbf{v} = \mathbf{v}_1^T \cdot \mathbf{D}^{N-1} \cdot \mathbf{v}_r = \sum_{i=1}^3 v_{1,i} v_{r,i} x_i^{N-1}. \quad (20)$$

where $\mathbf{D} = \mathbf{U}^{-1} \mathbf{T} \mathbf{U}$ is a diagonal matrix with eigenvalues x_i , the columns of \mathbf{U} are the right eigenvectors of \mathbf{T} , $\mathbf{v}_1^T = \mathbf{v}^T \cdot \mathbf{U}$ and $\mathbf{v}_r = \mathbf{U}^{-1} \mathbf{M}_{\text{TM}} \cdot \mathbf{v}$. By virtue of the Perron-Frobenius theorem one eigenvalue x_{max} is larger than the other eigenvalues and thus the free energy is in the thermodynamic limit dominated by x_{max} and reads

$$\mathcal{G} = -k_B T \ln \mathcal{Q}(N) \approx -k_B T N \ln x_{\text{max}}. \quad (21)$$

The transfer-matrix eigenvalues x_i and the poles λ_p of $\mathcal{Z}_{c=0}$ eq. (7) are related *via* $x_i = 1/\lambda_p$. As expected, the free energies from the transfer matrix approach eq. (21) and from the Poland-Scheraga approach for $c = 0$ and using the dominating singularity approximation eqs. (16) are identical in the limit $N \rightarrow \infty$. Clearly, for $c \neq 0$ the modified Poland-Scheraga approach yields new physics that deviates from the transfer-matrix results.

Although not pursued in this paper, the transfer matrix approach allows to calculate correlators. For example the probability $p_M(k, m)$ of a denatured region with k consecutive molten base pairs starting at base m is given by

$$p_M(k, m) = \mathcal{Q}(N)^{-1} \cdot \mathbf{v}^T \cdot \mathbf{T}^{m-2} (\mathbf{P}_B \mathbf{T} + \mathbf{P}_S \mathbf{T}) (\mathbf{P}_M \mathbf{T})^k (\mathbf{P}_B \mathbf{T} + \mathbf{P}_S \mathbf{T}) \mathbf{T}^{N-m-k-1} \mathbf{M}_{\text{TM}} \cdot \mathbf{v}. \quad (22)$$

The \mathbf{P}_i -matrices, which project a segment onto a certain state, are defined as

$$\mathbf{P}_B = \begin{pmatrix} 1 & 0 & 0 \\ 0 & 0 & 0 \\ 0 & 0 & 0 \end{pmatrix}, \quad \mathbf{P}_S = \begin{pmatrix} 0 & 0 & 0 \\ 0 & 1 & 0 \\ 0 & 0 & 0 \end{pmatrix}, \quad \text{and} \quad \mathbf{P}_M = \begin{pmatrix} 0 & 0 & 0 \\ 0 & 0 & 0 \\ 0 & 0 & 1 \end{pmatrix}. \quad (23)$$

IV. FORCE EXTENSION CURVES

The central quantity is $\mathcal{G}(F, T, N)$, the Gibbs free energy of a DNA chain with N base pairs, subject to a force F and temperature T . From $\mathcal{G}(F, T, N)$, obtained via the Legendre transform, eq. (13), the dominating singularity, eq. (16), or the exact transfer matrix partition function, eq. (20), we can calculate observables by performing appropriate derivatives. The number of segments in state $i = B, S, M$ is obtained by

$$N_i = \left. \frac{\partial \mathcal{G}}{\partial g_i} \right|_{T, N, F}. \quad (24)$$

The force extension curve is readily calculated *via*

$$x(F) = - \left. \frac{\partial \mathcal{G}}{\partial F} \right|_{T, N} = - \sum_{i=B, S, M} \frac{\partial \mathcal{G}}{\partial g_i} \frac{\partial g_i}{\partial F} = \sum_{i=B, S, M} N_i (x_i^{\text{WLC}}(F) + F \cdot l_i / \kappa_i) \quad (25)$$

where $x_i^{\text{WLC}}(F)$ is the stretching response of a worm-like chain and given explicitly in the supplementary information eq. (??).

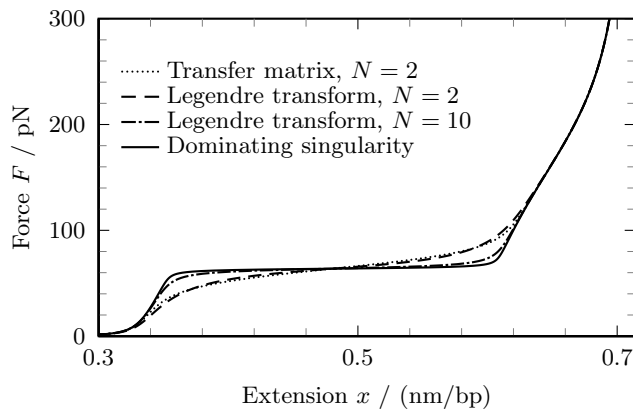


Figure 1: Comparison of force extension curves obtained by different methods for $c = 0$. The curve obtained *via* the exact transfer matrix calculation eq. (20) is already for $N = 2$ accurately reproduced by the approximate Legendre transformation eq. (13). The dominating singularity method eqs. (16) or – equivalently – (21) is strictly valid in the thermodynamic limit but agrees with the Legendre transform already for a modest value of $N = 10$. The units of the abscissa is extension per base pair (bp). Parameters for λ -DNA in the absence of DDP are used, see supporting material section ??.

A. Vanishing loop entropy, $c = 0$

In this section we compare the prediction for vanishing loop exponent $c = 0$ to experimental data and obtain estimates of the various parameters. We also demonstrate the equivalence of the grand canonical and canonical ensembles even for small chain length N .

In order to reduce the number of free fitting parameters we extract as many reasonable values from literature as possible. For the helical rise, the stretch modulus, and persistence length of B-DNA we use $l_B = 3.4 \text{ \AA}$, $\kappa_B = 1 \text{ nN}$, and $\xi_B = 48 \text{ nm}$ [52]. For the M-state, which is essentially single stranded DNA (ssDNA), *ab initio* calculations yield $l_M = 7.1 \text{ \AA}$ and $\kappa_M = 2 \cdot 9.4 \text{ nN}$ [53], where κ_M is valid for small forces $F < 400 \text{ pN}$ and the factor 2 accounts for the presence of two ssDNA strands. Our value for the stretch modulus is considerably larger than previous experimental fit estimates [4, 54] which might be related to the fact that experimental estimates depend crucially on the model used to account for conformational fluctuation effects; however, the actual value of κ_M is of minor importance for the stretching response, see supporting material. The persistence length of ssDNA is given by $\xi_M \approx 3 \text{ nm}$ [55]. It turns out that the quality of the fit as well as the values of the other fit parameters are not very sensitive to the exact value of the persistence length ξ_S and the stretch modulus κ_S of the S-state as long as $10 \text{ nm} \lesssim \xi_S \lesssim 50 \text{ nm}$ and κ_S is of the order of κ_M , see supporting material section ?. Therefore we set $\xi_S = 25 \text{ nm}$, which is an intermediate value between the persistence lengths of ssDNA and B-DNA, and $\kappa_S = \kappa_M = 2 \cdot 9.4 \text{ nN}$ [7]. The segment length of the S-state l_S will be a fit parameter.

The chemical potentials g_i^0 , $i = B, S, M$, account for the free energy of base pairing and, since we set the interaction energies between neighboring segments of the same type to zero, $V_{ii} = 0$, also for the free energy gain due to base pair stacking [56]. They also correct for the fact that the reference state of the three different WLCs, which is $x = 0$ in the Helmholtz ensemble (constant extension x), *cf.* eq. (??), is not the same as contour and persistence lengths differ for B-, S-, and molten M-DNA. We choose $g_B^0 = 0$ and treat g_S^0 and g_M^0 as fitting parameters.

Each of these parameters controls a distinct feature of the force-extension curve: The chemical potentials g_i^0 determine the critical forces, the segment lengths l_i affect the maximal extensions of each state and the off-diagonal V_{ij} control the cooperativity of the transitions, see supporting material section ?? for an illustration and section ?? for a summary of all parameter values.

1. Force extension curve

In fig. 1 force extension curves based on three different levels of approximation are compared, using the same parameters that we extracted from DNA stretching data as will be detailed below. It turns out that the force extension curve obtained *via* the Legendre transformation route eq. (13) (dashed line) is a very good approximation of the results obtained from the exact transfer matrix results eq. (20) (dotted line) already for $N = 2$. For $N = 10$ and larger virtually no differences between these two approaches are detectable. The deviations from the dominating singularity route eq. (16) (solid line), which gives a result independent of N , are somewhat larger. But one sees that

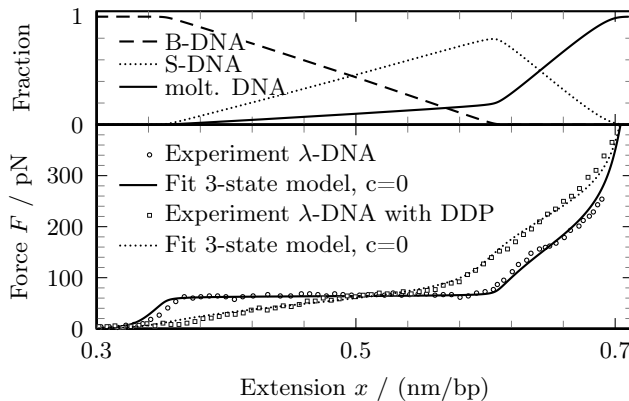


Figure 2: Bottom panel: Force extension curve of double-stranded λ -DNA with and without DDP. Symbols denote experimental data [20], lines are fits with the three-state model for $c = 0$. The main difference between the two curves is the lack of cooperativity in the BS-transition in the presence of DDP which we take into account by choosing vanishing interaction energies $V_{ij} = 0$, $i, j = B, S, M$. Top panel: Fraction N_i/N of segments in the different states as follows from eq. (24) in the absence of DDP.

already the Legendre transform for $N = 10$ (dash-dotted line) matches the dominating singularity result very closely. Therefore the use of the dominating singularity, eq. (16), or the largest transfer-matrix eigenvalue, eq. (21), is a very good approximation already for oligo-nucleotides and will be used in the rest of this work.

In fig. 2 experimental stretching curves of λ -DNA with and without DDP (cisplatin) are presented [20]. When B-DNA is converted into S-DNA or M-DNA the base stacking is interrupted which gives rise to an interfacial energy between B and S as well as between B and M of the order of the stacking energy [10, 11]. For untreated DNA, we use the value $V_{BS} = V_{SB} = V_{BM} = V_{MB} = 1.2 \cdot 10^{-20}$ J and show in the supplement that variations down to $0.8 \cdot 10^{-20}$ J do not change the resulting curves much. V_{SM} is presumably small as the stabilizing stacking interactions are already disrupted [7], we thus set $V_{SM} = V_{MS} = 0$ for the fits in fig. 2 – but we will come back to the issue of a non-zero V_{SM} later on. Cisplatin is thought to disrupt the stacking interaction between successive base pairs and thereby to reduce the cooperativity of the BS-transition. This fact we incorporate by setting all interfacial energies to zero, $V_{ij} = 0$, for DDP treated DNA. The three remaining undetermined parameters (l_S, g_S^0, g_M^0) have distinct consequences on the force-extension curve. The segment length l_S and the chemical potential g_S^0 determine the position of the BS-plateau with respect to the polymer extension and applied force, respectively, while the chemical potential g_M^0 controls the force at which the second transition appears. Fitting to experimental data is thus straightforward and yields for untreated λ -DNA $l_S = 6.1$ Å, $g_S^0 = 1.6 \cdot 10^{-20}$ J, $g_M^0 = 2.4 \cdot 10^{-20}$ J and for λ -DNA in the presence of DDP (cisplatin) $l_S = 6.0$ Å, $g_S^0 = 1.2 \cdot 10^{-20}$ J, $g_M^0 = 2.8 \cdot 10^{-20}$ J, see fig. 2. We also fit the number of monomers N and allow for an overall shift along the x -axis. The main difference between the two stretching curves is the cooperativity of the BS-transition, which is controlled by the interfacial energies V_{BS} and V_{BM} . Note that, although the over-stretching transition is quite sharp for DNA without DDP, it is not a phase transition in the strict statistical mechanics sense. A true phase transition arises only for $c > 1$, as will be shown in the next section. The fitted value of g_M^0 is about two times larger than typical binding energies [56] for pure DNA. As a possible explanation, we note that the force extension curve of DNA without DDP exhibits pronounced hysteresis (especially at higher force) which will increase the apparent binding energy due to dissipation effects [40]. Any statements as to the stability of S-DNA based on our fitting procedures are thus tentative. However, such complications are apparently absent in the presence of DDP [20] which rules out kinetic effects as the reason for our relatively high fit values of g_M^0 and the stability of S-DNA. Cisplatin most likely stabilizes base pairs due to cross-linking and thus shifts the subtle balance between B-, S-, and M-DNA. Therefore, the relative stability of B-, S-, and M-DNA is sensitively influenced by co-solute effects. We note that even with $c = 0$ a good fit of the data is possible. In the top panel of fig. 2 we show the fraction of segments in B-, S-, and M-states for untreated λ -DNA. There is a balanced distribution of bases in all three states across the full force range, in agreement with previous results [7].

B. Non-vanishing loop entropy, $c \neq 0$

We now turn to non-zero loop exponents $c \neq 0$ and in specific try to estimate c from the experimental stretching data. The partition function $\mathcal{Z}_{c \neq 0}$ in eq. (9) exhibits two types of singularities. First, simple poles at $\lambda = \lambda_p$, which

are the zeros of the denominator of eq. (9) and which are determined as the roots of the equation

$$-\frac{b_5 + b_6\lambda + b_7\lambda^2}{b_8\lambda + b_9\lambda^2} = \text{Li}_c(\lambda/\lambda_b) . \quad (26)$$

Second, a branch point that occurs at

$$\lambda = \lambda_b = e^{\beta g_M} . \quad (27)$$

The singularity with the smallest modulus is the dominant one [1, 51], and we define the critical force F_c as the force where both equations, eq. (26) and (27), hold simultaneously. For $c \leq 1$ the dominant singularity is always given by the pole λ_p and thus no phase transition is possible. For $1 < c \leq 2$ a continuous phase transition occurs. By expanding eq. (26) around F_c one can show that all derivatives of the free energy up to order n are continuous, where $n \in \mathbb{N}$ is defined as the largest integer with $n < (c - 1)^{-1}$ [3]. For instance, $c = 3/2$ leads to a kink in the force extension curve. For $c = 1.2$ this leads to a kink in $x'''(F)$. If $c > 2$ the transition becomes first order and the force extension curve exhibits a discontinuity at $F = F_c$. In fig. 3a we plot force extension curves for different values of the loop exponent c with all other parameter fixed at the values fitted for untreated DNA. It is seen that finite c leads to changes of the force extension curves only at rather elevated forces. In order to see whether a finite c improves the comparison with the experiment and whether it is possible to extract the value of c from the data, we in fig. 3b compare the untreated DNA data with a few different model calculations for which we keep the parameters $l_S, g_S^0, g_M^0, V_{BS}, V_{BM}$ fixed at the values used for the fit with $c = 0$ in fig. 2. Allowing for finite c but fixing a zero domain wall energy between S- and M-regions, $V_{SM} = 0$, leads to an optimal exponent $c = 0.6$ and slightly improves the fit to the data which show the onset of a plateau at a force of about 100 pN. The same effect, however, can be produced by fixing $c = 0$ and allowing for a finite V_{SM} , which yields the optimal value of $V_{SM} = 1.1 \cdot 10^{-21}$ J. Finally, fixing $V_{SM} = 1.1 \cdot 10^{-21}$ J and optimizing c yields in this case $c = 0.3$ and perfect agreement with the experimental data. However, the significance of this improvement is not high, as the experimental data are quite noisy and possibly plagued by kinetic effects. What the various curves illustrate quite clearly, however, is that a non-zero exponent c leads to modifications of the stretching curves that are similar to the effects of a non-vanishing domain wall energy V_{SM} . Although V_{SM} should be considerably smaller than V_{BM} or V_{BS} , a finite value of $V_{SM} = 1.1 \cdot 10^{-21}$ J as found in the fit is reasonable and cannot be ruled out on general grounds. The maximal value of c is obtained for vanishing V_{SM} and amounts to about $c = 0.6$. A value of $c = 2.1$, which would be expected based on the entropy of internal DNA loops [3], on the other hand does not seem compatible with the experimental data, as follows from fig. 3a. This might have to do with the presence of nicks. Nicks in the DNA drastically change the topology of loops and result in a reduced loop exponent which is $c = 0$ for an ideal polymer and 0.092 for a self avoiding polymer [3]. Therefore, the low value of c we extract from experimental data might be a signature of nicked DNA. Additional effects such as salt or co-solute binding to loops are also important. Therefore c can be viewed as a heuristic parameter accounting for such non-universal effects as well. We note in passing that c only slightly affects the BS-transition, as seen in fig. 3a.

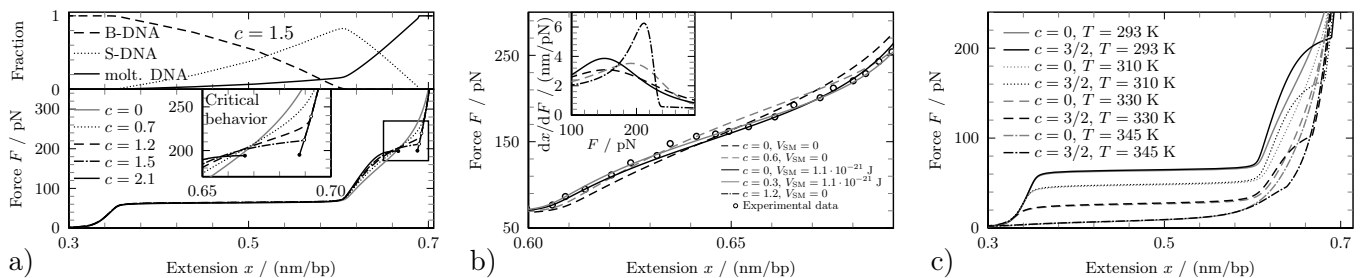


Figure 3: Various force-extension curves of the three-state model with fit parameters for λ -DNA without DDP. **a)** Lower panel: Force extension curves for different values of the loop exponent c , showing no phase transition ($c \leq 1$), a continuous ($1 < c \leq 2$), or a first order phase transition ($c > 2$). The critical forces are denoted by open circles. The inset is a magnification of the region around the transition. Upper panel: Fraction of bases in the three states for $c = 3/2$. The critical transition, above which all bases are in the molten M-state, is discerned as a kink in the curves. **b)** Comparison of experimental data (circles) and theory for $c \neq 0$. The curve for $c = 0$ and $V_{SM} = 0$, already shown in fig. 2, is obtained by fitting l_S , g_S^0 , g_M^0 to the experimental data, the values of which are kept fixed for all curves shown. The curve for $V_{SM} = 0$ and $c = 0.6$ results by fitting c and slightly improves the fit quality. The curve $c = 0$ and $V_{SM} = 1.1 \cdot 10^{-21}$ J is obtained by fitting V_{SM} . The curve for $V_{SM} = 1.1 \cdot 10^{-21}$ J and $c = 0.3$ is obtained by fitting c and keeping V_{SM} fixed. The inset shows the first derivative of $x(F)$ and illustrates that increasing c leads to a growing asymmetry around the transition region. **c)** Temperature dependence of the force extension curves. Increasing temperature leads to a decrease of the BS-plateau force. In the presence of a true denaturing transition, i.e. for $c > 1$, the critical force F_c decreases with increasing temperature and for $F > F_c$ the force extension curve follows a pure WLC behavior.

V. FINITE TEMPERATURE EFFECTS

The temperature dependence of all parameters is chosen such that the force extension curves at $T = 20^\circ\text{C}$ that were discussed up to now remain unchanged. The persistence lengths are modeled as $\xi_i(T) = \xi_i \cdot (T/293\text{ K})^{-1}$. The S-state free energy is split into enthalpic and entropic parts as $g_S^0(T) = \tau_S(h_S - T s_S)$ where we use $h_S = 7.14 \cdot 10^{-20}$ J and $s_S = 1.88 \cdot 10^{-22}$ J/K from Clausen-Schaumann et al. [19]. The correction factor $\tau_S = 0.98$ accounts for slight differences in the experimental setups and is determined such that $g_S^0(T = 20^\circ\text{C})$ equals the previously fitted value. The molten state energy $g_M^0(T) = (h_M - T s_M)$ is also chosen such that $g_M^0(T = 20^\circ\text{C})$ agrees with the previous fit value and that the resulting denaturing temperature in the absence of force agrees with experimental data. Assuming a melting temperature of $T_c = 348$ K for λ -DNA [57], we obtain $g_M^0(T) = 1.5 \cdot 10^{-19}$ J - $T \cdot 4.2 \cdot 10^{-22}$ J/K for $c = 0$ and $g_M^0(T) = 1.6 \cdot 10^{-19}$ J - $T \cdot 4.6 \cdot 10^{-22}$ J/K for $c = 3/2$. In fig. 3c we plot a few representative stretching curves for different temperatures. It is seen that increasing temperature lowers the BS-plateau and makes this transition less cooperative. Differences between $c = 0$ and $c = 3/2$ are only observed at elevated forces, where for $c = 3/2$ one encounters a singularity characterized by a kink in the extension curves.

For $c > 1$ the critical force F_c is defined as the force where the pole and the branch point coincide and eqs. (26) and (27) are simultaneously satisfied. The phase boundary in the force-temperature plane is thus defined by

$$-\frac{b_5 + b_6 \lambda_b + b_7 \lambda_b^2}{b_8 \lambda_b + b_9 \lambda_b^2} = \zeta(c), \quad (28)$$

where b_i and λ_b depend on T and F and $\zeta(c) = \text{Li}_c(1)$ is the Riemann zeta function. The phase boundary $F_c(T)$ for $c = 3/2$ is shown in fig. 4 and agrees qualitatively with the experimental data of ref. [14]. For exponents $c < 1$ no true phase transition exists. We therefore define crossover forces as the force at which half of the segments are in the molten state or in the B-state, i.e. $N_M/N = 1/2$ or $N_B/N = 1/2$. In fig. 4 we show these lines for both $c = 0$ and $c = 3/2$. Note that the parameters for the $c = 0$ case have been adjusted so that $N_M/N = 1/2$ at $T = 348$ K and $F = 0$. The broken lines on which $N_B/N = 1/2$ for $c = 0$ and $c = 3/2$ are virtually the same, showing again that loop entropy is irrelevant for the BS-transition. The S-state is populated in the area between the $N_B/N = 1/2$ and $N_M/N = 1/2$ lines, which for $T > 330$ K almost coalesce, meaning that at elevated temperatures the S-state is largely irrelevant. Force-induced re-entrance at constant temperature is found in agreement with previous two-state models [30, 35]. Re-entrance at constant force as found for a Gaussian model [30] is not reproduced, in agreement with results for a non-extensible chain [35].

As we have shown so far, a non-zero loop exponent c only slightly improves the fit of the experimental stretching data and the optimal value found is less than unity. This at first sight seems at conflict with recent theoretical work that argued that a loop exponent larger than $c = 2$ is needed in order to produce denaturation curves (at zero force) that resemble experimental curves in terms of the steepness or cooperativity of the transition [3]. To look into

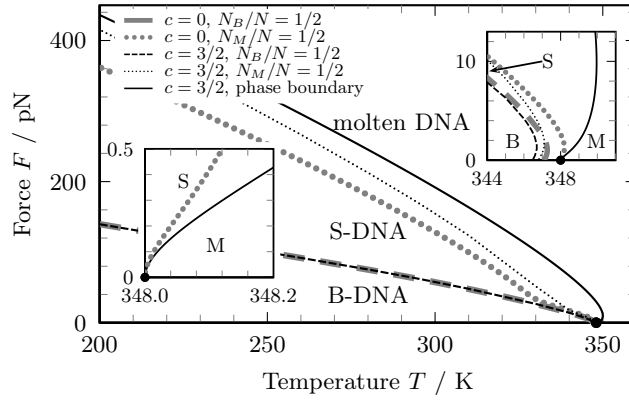


Figure 4: The solid line shows the critical force F_c for $c = 3/2$, at which a singularity occurs according to eq. (28). Phase boundaries for $c = 0$ (thick lines) and $c = 3/2$ (thin lines) are defined by $N_M/N = 0.5$ (dotted) and $N_B/N = 0.5$ (dashed). The melting temperature T_c is denoted by the dot. The insets show the behavior of the phase boundaries near the melting temperature, $F \propto \sqrt{T_c - T}$. Parameters for λ -DNA without DDP are used.

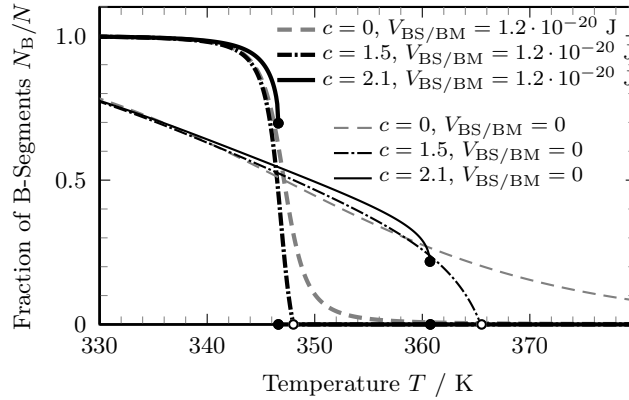


Figure 5: Relative fraction of segments in the B-state, N_B/N , as a function of temperature for different loop exponents $c = 0, 1.5, 2.1$ and for finite BS interfacial energy $V_{BS} = V_{BM} = 1.2 \cdot 10^{-20}$ J (bold lines) and for $V_{BS} = V_{BM} = 0$ (thin lines). Circles indicate the positions of the phase transition. For all curves parameters for λ -DNA without DDP have been used, $g_M^0(T) = 1.5 \cdot 10^{-19}$ J $- T \cdot 4.2 \cdot 10^{-22}$ J/K for $c = 0$ and $g_M^0(T) = 1.6 \cdot 10^{-19}$ J $- T \cdot 4.6 \cdot 10^{-22}$ J/K for $c > 0$.

this issue, we plot in fig. 5 the fraction of native base pairs, N_B/N as a function of temperature for zero force and different parameters. As soon as the domain-wall energies V_{BS} and V_{BM} are finite, the transition is quite abrupt, even for vanishing exponent c . Therefore even loop exponents $c < 1$ yield melting curves which are consistent with experimental data, where melting occurs over a range of the order of 10 K [57, 58].

VI. CONCLUSIONS

The fact that the domain-wall energy due to the disruption of base pair stacking, V_{BS} and V_{BM} , and the loop entropy embodied in the exponent c , give rise to similar trends and sharpen the melting transition has been realized and discussed before [9, 58]. The present three-state model and the simultaneous description of experimental data where the denaturation is induced by application of force and by temperature allows to disentangle the influence of these two important effects. By the application of a force, the de-stacking and the loop formation occur subsequently, allowing to fit both parameters separately. As our main finding, we see that for a finite domain-wall energy $V_{BS} = V_{BM}$, the additional influence of the loop exponent on the force stretching curves and the denaturation curves is small. In fact, the optimal value for c turns out to be of the order of $c \approx 0.3 - 0.6$, even if we choose a vanishing value $V_{SM} = 0$. This estimate for c is smaller than previous estimates. One reason for this might be nicks in the DNA. So it would be highly desirable to redo stretching experiments with un-nicked DNA from which the value of c under tension could be determined. A second transition at high forces of about $F \simeq 200$ pN which is seen in the experimental data used in the paper, inevitably leads via the fitting within our three-state model to an intermediate S-DNA state. But we stress

that the occurrence of such an intermediate S-state depends on the fine-tuning of all model parameters involved, which suggests that in experiments the S-state stability should also sensitively depend on the precise conditions. One drawback of the current model is that sequence effects are not taken into account. This means that our fitted parameters have to be interpreted as coarse-grained quantities which average over sequence disorder. Calculations with explicit sequences have been done for short DNA strands but should in the future be doable for longer DNA as well.

VII. ACKNOWLEDGMENTS

The authors express their gratitude to Hauke Clausen-Schaumann and Rupert Krautbauer for providing the experimental data and helpful comments and thank Ralf Metzler, Matthias Erdmann, and Dominik Ho for fruitful discussions. Financial support comes from the DFG *via* grants NE 810/7 and SFB 863. T.R.E. acknowledges support from the *Elitenetzwerk Bayern* within the framework of *CompInt*.

-
- [1] Poland, D., and H. A. Scheraga, 1966. Phase Transitions in One Dimension and the Helix – Coil Transition in Polyamino Acids. *J. Chem. Phys.* 45:1456–1463.
 - [2] Poland, D., and H. A. Scheraga, 1966. Occurrence of a Phase Transition in Nucleic Acid Models. *J. Chem. Phys.* 45:1464–1469.
 - [3] Kafri, Y., D. Mukamel, and L. Peliti, 2002. Melting and Unzipping of DNA. *Eur. Phys. J. B* 27:135–146.
 - [4] Smith, S. B., Y. J. Cui, and C. Bustamante, 1996. Overstretching B-DNA: The Elastic Response of Individual Double-stranded and Single-stranded DNA Molecules. *Science* 271:795–799.
 - [5] Bensimon, D., A. J. Simon, V. Croquette, and A. Bensimon, 1995. Stretching DNA with a Receding Meniscus: Experiments and Models. *Phys. Rev. Lett.* 74:4754–4757.
 - [6] Cluzel, P., A. Lebrun, C. Heller, R. Lavery, J.-L. Viovy, D. Chatenay, and F. Caron, 1996. DNA: An Extensible Molecule. *Science* 271:792794.
 - [7] Cocco, S., J. Yan, J.-F. Léger, D. Chatenay, and J. F. Marko, 2004. Overstretching and force-driven strand separation of double-helix DNA. *Phys. Rev. E* 70:011910.
 - [8] Léger, J. F., G. Romano, A. Sarkar, J. Robert, L. Bourdieu, D. Chatenay, and J. F. Marko, 1999. Structural Transitions of a Twisted and Stretched DNA Molecule. *Phys. Rev. Lett.* 83:1066.
 - [9] Whitelam, S., S. Pronk, and P. L. Geissler, 2008. There and (Slowly) Back Again: Entropy-Driven Hysteresis in a Model of DNA Overstretching. *Biophys. J.* 94:2452–2469.
 - [10] Konrad, M., and J. Bolonick, 1996. Molecular Dynamics Simulation of DNA Stretching Is Consistent with the Tension Observed for Extension and Strand Separation and Predicts a Novel Ladder Structure. *J. Am. Chem. Soc.* 118:10989–10994.
 - [11] Kosikov, K. M., A. A. Gorin, V. B. Zhurkin, and W. K. Olson, 1999. DNA stretching and compression: large-scale simulations of double helical structures. *J. Mol. Biol.* 289:1301–1326.
 - [12] Li, H., and T. Gisler, 2009. Overstretching of a 30 bp DNA duplex studied with steered molecular dynamics simulation: Effects of structural defects on structure and force-extension relation. *Eur. Phys. J. E* 30:325–332.
 - [13] Lebrun, A., and R. Lavery, 1996. Modelling extreme stretching of DNA. *Nucleic Acids Res.* 24:2260–2267.
 - [14] Williams, M. C., J. R. Wenner, I. Rouzina, and V. A. Bloomfield, 2001. Entropy and Heat Capacity of DNA Melting from Temperature Dependence of Single Molecule Stretching. *Biophys. J.* 80:1932–1939.
 - [15] Rouzina, I., and V. A. Bloomfield, 2001. Force-Induced Melting of the DNA Double Helix 1. Thermodynamic Analysis. *Biophys. J.* 80:882–893.
 - [16] Shokri, L., M. J. McCauley, I. Rouzina, and M. C. Williams, 2008. DNA Overstretching in the Presence of Glyoxal: Structural Evidence of Force-Induced DNA Melting. *Biophys. J.* 95:1248–1255.
 - [17] van Mameren, J., P. Gross, G. Farge, P. Hooijman, M. Modesti, M. Falkenberg, G. J. L. Wuite, and E. J. G. Peterman, 2009. Unraveling the structure of DNA during overstretching by using multicolor, single-molecule fluorescence imaging. *Proc. Natl. Acad. Sci. U. S. A.* 106:18231–18236.
 - [18] Rief, M., H. Clausen-Schaumann, and H. E. Gaub, 1999. Sequence-dependent mechanics of single DNA molecules. *Nat. Struct. Biol.* 6:346–349.
 - [19] Clausen-Schaumann, H., M. Rief, C. Tolksdorf, and H. E. Gaub, 2000. Mechanical Stability of Single DNA Molecules. *Biophys. J.* 78:1997–2007.
 - [20] Krautbauer, R., H. Clausen-Schaumann, and H. E. Gaub, 2000. Cisplatin Changes the Mechanics of Single DNA Molecules. *Angew. Chem. Int. Edit.* 39:3912–3915.
 - [21] Baumann, C. G., S. B. Smith, V. A. Bloomfield, and C. Bustamante, 1997. Ionic effects on the elasticity of single DNA molecules. *Proc. Natl. Acad. Sci. U. S. A.* 94:6185–6190.
 - [22] Piana, S., 2005. Structure and energy of a DNA dodecamer under tensile load. *Nucleic Acids Res.* 33:7029–7038.
 - [23] Cocco, S., J. F. Marko, and R. Monasson, 2002. Theoretical models for single-molecule DNA and RNA experiments: from elasticity to unzipping. *C. R. Phys.* 3:569–584.

- [24] Peyrard, M., S. Cuesta-López, and G. James, 2008. Modelling DNA at the mesoscale: a challenge for nonlinear science? *Nonlinearity* 21:T91–T100.
- [25] Wartell, R. M., and A. S. Benight, 1985. Thermal denaturation of DNA molecules: A comparison of theory with experiment. *Phys. Rep.* 126:67–107.
- [26] Cizeau, P., and J.-L. Viovy, 1997. Modeling Extreme Extension of DNA. *Biopolymers* 42:383–385.
- [27] Ahsan, A., J. Rudnick, and R. Bruinsma, 1998. Elasticity Theory of the B-DNA to S-DNA Transition. *Biophys. J.* 74:132–137.
- [28] Storm, C., and P. C. Nelson, 2003. Theory of high-force DNA stretching and overstretching. *Phys. Rev. E* 67:051906.
- [29] Marko, J. F., 1998. DNA under high tension: Overstretching, undertwisting, and relaxation dynamics. *Phys. Rev. E* 57:2134.
- [30] Hanke, A., M. G. Ochoa, and R. Metzler, 2008. Denaturation Transition of Stretched DNA. *Phys. Rev. Lett.* 100:018106.
- [31] Rudnick, J., and T. Kuriabova, 2008. Effect of external stress on the thermal melting of DNA. *Phys. Rev. E* 77:051903.
- [32] Garel, T., and H. Orland, 2004. Generalized Poland-Scheraga Model for DNA Hybridization. *Biopolymers* 75:453–467.
- [33] Blake, R. D., J. W. Bizzaro, J. Blake, G. R. Day, S. G. Delcourt, J. Knowles, K. A. Marx, and J. SantaLucia, Jr, 1999. Statistical mechanical simulation of polymeric DNA melting with MELTSIM. *Bioinformatics* 15:370–375.
- [34] Carlon, E., E. Orlandini, and A. L. Stella, 2002. Roles of Stiffness and Excluded Volume in DNA Denaturation. *Phys. Rev. Lett.* 88:198101.
- [35] Rahi, S. J., M. P. Hertzberg, and M. Kardar, 2008. Melting of persistent double-stranded polymers. *Phys. Rev. E* 78:051910.
- [36] Palmeri, J., M. Manghi, and N. Destainville, 2007. Thermal Denaturation of Fluctuating DNA Driven by Bending Entropy. *Phys. Rev. Lett.* 99:088103.
- [37] Jeon, J.-H., W. Sung, and F. H. Ree, 2006. A semiflexible chain model of local denaturation in double-stranded DNA. *J. Chem. Phys.* 124:164905.
- [38] Peyrard, M., 2004. Nonlinear dynamics and statistical physics of DNA. *Nonlinearity* 17:R1–R40.
- [39] Cule, D., and T. Hwa, 1997. Denaturation of Heterogeneous DNA. *Phys. Rev. Lett.* 79:2375.
- [40] Ho, D., J. L. Zimmermann, F. A. Dehmelt, U. Steinbach, M. Erdmann, P. Severin, K. Falter, and H. E. Gaub, 2009. Force-Driven Separation of Short Double-Stranded DNA. *Biophys. J.* 97:3158–3167.
- [41] Bar, A., Y. Kafri, and D. Mukamel, 2007. Loop Dynamics in DNA Denaturation. *Phys. Rev. Lett.* 98:038103.
- [42] Marko, J. F., and E. D. Siggia, 1995. Stretching DNA. *Macromolecules* 28:8759–8770.
- [43] Netz, R. R., 2001. Strongly Stretched Semiflexible Extensible Polyelectrolytes and DNA. *Macromolecules* 34:7522–7529.
- [44] Livadaru, L., R. R. Netz, and H. J. Kreuzer, 2003. Stretching Response of Discrete Semiflexible Polymers. *Macromolecules* 36:3732–3744.
- [45] Odijk, T., 1995. Stiff Chains and Filaments under Tension. *Macromolecules* 28:7016–7018.
- [46] Einert, T. R., P. Näger, H. Orland, and R. R. Netz, 2008. Impact of Loop Statistics on the Thermodynamics of RNA Folding. *Phys. Rev. Lett.* 101:048103.
- [47] de Gennes, P.-G., 1979. Scaling Concepts in Polymer Physics. Cornell University Press.
- [48] Duplantier, B., 1986. Polymer Network of Fixed Topology: Renormalization, Exact Critical Exponent γ in two Dimensions, and $d = 4 - \epsilon$. *Phys. Rev. Lett.* 57:941–944.
- [49] Erdélyi, A., 1953. Higher Transcendental Functions, volume 1. McGraw-Hill.
- [50] Arfken, G. B., and H. J. Weber, 2001. Mathematical Methods for Physicists. Academic Press, fifth edition.
- [51] Flajolet, P., and A. Odlyzko, 1990. Singularity Analysis of Generating Functions. *SIAM Discret. Math.* 3:216–240.
- [52] Wenner, J. R., M. C. Williams, I. Rouzina, and V. A. Bloomfield, 2002. Salt Dependence of the Elasticity and Overstretching Transition of Single DNA Molecules. *Biophys. J.* 82:3160–3169.
- [53] Hugel, T., M. Rief, M. Seitz, H. E. Gaub, and R. R. Netz, 2005. Highly Stretched Single Polymers: Atomic-Force-Microscope Experiments Versus Ab-Initio Theory. *Phys. Rev. Lett.* 94:048301.
- [54] Dessinges, M.-N., B. Maier, Y. Zhang, M. Peliti, D. Bensimon, and V. Croquette, 2002. Stretching Single Stranded DNA, a Model Polyelectrolyte. *Phys. Rev. Lett.* 89:248102.
- [55] Murphy, M., I. Rasnik, W. Cheng, T. M. Lohman, and T. Ha, 2004. Probing Single-Stranded DNA Conformational Flexibility Using Fluorescence Spectroscopy. *Biophys. J.* 86:2530–2537.
- [56] SantaLucia, J., Jr., 1998. A Unified View of Polymer, Dumbbell, and Oligonucleotide DNA Nearest-Neighbor Thermodynamics. *Proc. Natl. Acad. Sci. U. S. A.* 95:1460–1465.
- [57] Gotoh, O., Y. Husimi, S. Yabuki, and A. Wada, 1976. Hyperfine structure in melting profile of bacteriophage lambda DNA. *Biopolymers* 15:655–670.
- [58] Blossey, R., and E. Carlon, 2003. Reparametrizing the loop entropy weights: Effect on DNA melting curves. *Phys. Rev. E* 68:061911.

Supporting material

A three-state model with loop entropy for the over-stretching transition of DNA

Thomas R. Einert,^{1,*} Douglas B. Staple,^{2,3} Hans-Jürgen Kreuzer,² and Roland R. Netz^{1,†}

¹*Physik Department, Technische Universität München, 85748 Garching, Germany*

²*Department of Physics and Atmospheric Science, Dalhousie University, Halifax, B3H 3J5 Canada*

³*Max-Planck-Institut für Physik komplexer Systeme, 01187 Dresden, Germany*

(Dated: November 10, 2018)

The supporting material shows the calculation of the of Gibbs free energy $g_i^{\text{WLC}}(F)$ of one worm-like chain segment subject to a force F . Additionally the explicit form of the grand canonical partition function \mathcal{Z} is given. The loop exponent of an ideal polymer is derived and effects of self-avoidance on the loop exponent are discussed. We illustrate that different model parameters are linked to certain features of the force extension curve. Tables with all parameters used in the main paper are given at the end of this document.

Contents

A. Gibbs free energy of a worm-like chain	1
B. Explicit form of the grand canonical partition function	2
C. Origin of the logarithmic loop entropy	2
D. Effect of parameters on features of the force-extension curve	3
E. Tables with model parameters	6
References	6

A. GIBBS FREE ENERGY OF A WORM-LIKE CHAIN

To calculate the worm-like chain Gibbs free energy $g_i^{\text{WLC}}(F)$, we first calculate the Helmholtz free energy $H_i^{\text{WLC}}(x)$ of a worm-like chain (WLC) in the fixed extension ensemble (Helmholtz ensemble). After that we Legendre transform $H_i^{\text{WLC}}(x)$ in order to obtain $G_i^{\text{WLC}}(F)$, which is the thermodynamic potential of a WLC in the fixed force ensemble (Gibbs ensemble). As we will see, $G_i^{\text{WLC}}(F)$ is extensive with respect to the chain's contour length nl_i , l_i is the length of one segment, and thus we can define the Gibbs free energy per segment $g_i^{\text{WLC}}(F) = G_i^{\text{WLC}}(F)/n$. We introduce the dimensionless variables

$$\tilde{x}_i = \frac{x}{nl_i}, \quad \tilde{F}_i = F \cdot \beta \xi_i, \quad \tilde{H}_i^{\text{WLC}} = H_i^{\text{WLC}} \cdot \frac{\beta \xi_i}{nl_i}, \quad \tilde{G}_i^{\text{WLC}} = G_i^{\text{WLC}} \cdot \frac{\beta \xi_i}{nl_i}, \quad i = \text{B, S, M}, \quad (\text{S1})$$

where ξ_i is the persistence length of DNA in state $i = \text{B, S, M}$. The interpolation formula of Marko and Siggia [1] for the force extension curve of the WLC

$$\tilde{F}_i(\tilde{x}_i) = \frac{1}{4(1 - \tilde{x}_i)^2} + \tilde{x}_i - \frac{1}{4} \quad (\text{S2})$$

is used to calculate the free energy in the Helmholtz ensemble

$$\tilde{H}_i^{\text{WLC}}(\tilde{x}) = \int_0^{\tilde{x}} \tilde{F}(\tilde{x}') d\tilde{x}' + \tilde{H}_{i,0}^{\text{WLC}} = \frac{\tilde{x}^2(2\tilde{x} - 3)}{4(\tilde{x} - 1)} + \tilde{H}_{i,0}^{\text{WLC}}. \quad (\text{S3})$$

*E-mail: einert@ph.tum.de

†E-mail: netz@ph.tum.de

$\tilde{H}_{i,0}^{\text{WLC}}$ is a free energy offset that accounts for the fact that even in the absence of an external force the free energies of chains consisting of B-, S-, or M-segments are not the same. In fact, this constant is not easy to calculate but can be dropped in the following since it can be adsorbed into the free energy contributions g_i^0 , cf. eq. (??) in the main text.

Now, we invert eq. (S2)

$$\tilde{x}_i(\tilde{F}_i) = 1 - \left[\frac{\frac{4\tilde{F}_i}{3} - 1}{\left(2 + \sqrt{4 - \left(\frac{4\tilde{F}_i}{3} - 1\right)^3}\right)^{1/3}} + \left(2 + \sqrt{4 - \left(\frac{4\tilde{F}_i}{3} - 1\right)^3}\right)^{1/3} \right]^{-1} \quad (\text{S4})$$

and perform a Legendre transformation to obtain the Gibbs free energy of a WLC in the Gibbs ensemble

$$\tilde{G}_i^{\text{WLC}}(\tilde{F}_i) = \tilde{H}_i^{\text{WLC}}(\tilde{x}_i(\tilde{F}_i)) - \tilde{F}_i \cdot \tilde{x}_i(\tilde{F}_i). \quad (\text{S5})$$

Eqs. (S1) and (S5) lead to

$$g_i^{\text{WLC}}(F) = \frac{1}{n} \cdot \frac{nl_i}{\beta\xi_i} \cdot \tilde{G}^{\text{WLC}}(F\beta\xi_i) = \frac{l_i}{\beta\xi_i} \left(\frac{\tilde{x}_i(F\beta\xi_i)^2 (2\tilde{x}_i(F\beta\xi_i) - 3)}{4(\tilde{x}_i(F\beta\xi_i) - 1)} - F\beta\xi_i \cdot \tilde{x}_i(F\beta\xi_i) \right), \quad (\text{S6})$$

with $\tilde{x}_i(\tilde{F}_i)$ from eq. (S4).

B. EXPLICIT FORM OF THE GRAND CANONICAL PARTITION FUNCTION

In the main text the expression

$$\mathcal{Z} = \sum_{k=0}^{\infty} \mathbf{v}^T \cdot (\mathbf{M}_{\text{PS}} \mathbf{V}_{\text{PS}})^k \mathbf{M}_{\text{PS}} \cdot \mathbf{v} = \mathbf{v}^T \cdot (\mathbf{1} - \mathbf{M}_{\text{PS}} \mathbf{V}_{\text{PS}})^{-1} \mathbf{M}_{\text{PS}} \cdot \mathbf{v}, \quad (\text{S7})$$

has been derived for the grand canonical partition function. The matrices are given by

$$\mathbf{M}_{\text{PS}} = \begin{pmatrix} \mathcal{Z}_{\text{B}} & 0 & 0 \\ 0 & \mathcal{Z}_{\text{S}} & 0 \\ 0 & 0 & \mathcal{Z}_{\text{M}} \end{pmatrix}, \quad \mathbf{V}_{\text{PS}} = \begin{pmatrix} 0 & e^{-\beta V_{\text{BS}}} & e^{-\beta V_{\text{BM}}} \\ e^{-\beta V_{\text{SB}}} & 0 & e^{-\beta V_{\text{SM}}} \\ e^{-\beta V_{\text{MB}}} & e^{-\beta V_{\text{MS}}} & 0 \end{pmatrix}, \quad \mathbf{v} = \begin{pmatrix} 1 \\ 1 \\ 1 \end{pmatrix}. \quad (\text{S8})$$

$\mathbf{1}$ is the unity matrix. Evaluating eq. (S7) yields the grand canonical partition function of the three-state model

$$\begin{aligned} \mathcal{Z} = & \left[\mathcal{Z}_{\text{B}} + \mathcal{Z}_{\text{S}} + \mathcal{Z}_{\text{M}} + (e^{-\beta V_{\text{BS}}} + e^{-\beta V_{\text{SB}}}) \mathcal{Z}_{\text{B}} \mathcal{Z}_{\text{S}} + (e^{-\beta V_{\text{SM}}} + e^{-\beta V_{\text{MS}}}) \mathcal{Z}_{\text{S}} \mathcal{Z}_{\text{M}} + (e^{-\beta V_{\text{MB}}} + e^{-\beta V_{\text{BM}}}) \mathcal{Z}_{\text{M}} \mathcal{Z}_{\text{B}} \right. \\ & + \left(e^{-\beta(V_{\text{BS}}+V_{\text{SM}})} + e^{-\beta(V_{\text{SM}}+V_{\text{MB}})} + e^{-\beta(V_{\text{MB}}+V_{\text{BS}})} + e^{-\beta(V_{\text{BM}}+V_{\text{MS}})} + e^{-\beta(V_{\text{MS}}+V_{\text{SB}})} + e^{-\beta(V_{\text{SB}}+V_{\text{BM}})} \right. \\ & \left. \left. - e^{-\beta(V_{\text{BS}}+V_{\text{SB}})} - e^{-\beta(V_{\text{SM}}+V_{\text{MS}})} - e^{-\beta(V_{\text{MB}}+V_{\text{BM}})} \right) \mathcal{Z}_{\text{B}} \mathcal{Z}_{\text{S}} \mathcal{Z}_{\text{M}} \right] \\ & \times \left[\mathbf{1} - e^{-\beta(V_{\text{BS}}+V_{\text{SB}})} \mathcal{Z}_{\text{B}} \mathcal{Z}_{\text{S}} - e^{-\beta(V_{\text{SM}}+V_{\text{MS}})} \mathcal{Z}_{\text{S}} \mathcal{Z}_{\text{M}} - e^{-\beta(V_{\text{MB}}+V_{\text{BM}})} \mathcal{Z}_{\text{M}} \mathcal{Z}_{\text{B}} \right. \\ & \left. - \left(e^{-\beta(V_{\text{BS}}+V_{\text{SM}}+V_{\text{MB}})} + e^{-\beta(V_{\text{BM}}+V_{\text{MS}}+V_{\text{SB}})} \right) \mathcal{Z}_{\text{B}} \mathcal{Z}_{\text{S}} \mathcal{Z}_{\text{M}} \right]^{-1}, \quad (\text{S9}) \end{aligned}$$

which depends on the grand canonical partition functions \mathcal{Z}_i of the different regions.

C. ORIGIN OF THE LOGARITHMIC LOOP ENTROPY

In the simplest case a polymer can be described as an ideal random walk with step length b in $d = 3$ dimensions. When speaking of polymers b is also called *Kuhn length*. Let us first consider a one-dimensional random walk. The

probability to be after N steps at point $x = nb$ is given by the binomial distribution

$$P(x) = \frac{N!}{((N+n)/2)!((N-n)/2)!} \cdot p^{(N+n)/2} \cdot (1-p)^{(N-n)/2} = \binom{N}{(N+n)/2} \cdot p^{(N+n)/2} \cdot (1-p)^{(N-n)/2}, \quad (\text{S10})$$

where $p = 1/2$ is the probability to move to the right and $(1-p)$ the probability to move to the left. By virtue of the central limit theorem the binomial distribution can be approximated by the normal distribution if N is large

$$P(x) \simeq \frac{1}{\sqrt{Nb^2 2\pi}} e^{-\frac{1}{2} \frac{x^2}{Nb^2}}. \quad (\text{S11})$$

Now, we consider a random walk in three dimensions, where there are $N/3$ steps in each spatial direction. Since the steps in each of the three directions are independent from each other the probability distribution for being at point $\mathbf{R} = (x, y, z)$ after N steps is

$$P(\mathbf{R}) = P(x)P(y)P(z) = \frac{1}{(Nb^2 2\pi/3)^{3/2}} e^{-\frac{3}{2} \frac{R^2}{Nb^2}}. \quad (\text{S12})$$

The probability of a closed random walk, *i. e.* a loop, is the probability to return to the origin after N steps

$$P(0) = \frac{1}{(Nb^2 2\pi/3)^{3/2}}. \quad (\text{S13})$$

The entropy difference between an ideal polymer forming a loop and an unconstrained polymer is therefore given by

$$\Delta S_{\text{loop}}(N) = k_B \ln P(0) \sim k_B \ln N^{-c}, \quad (\text{S14})$$

where we introduced the *loop exponent* $c = c_{\text{ideal}} = d/2 = 3/2$ [2].

If one considers now self-avoiding polymers the loop exponent increases, $c_{\text{SAW}} = d\nu \simeq 1.76$ with $\nu \simeq 0.588$ in $d = 3$ dimensions [2]. Hence the entropic penalty for closing a loop increases. However, helices emerging from the loop increase c further. In the asymptotic limit of long helical sections, renormalization group predicts $c_l = d\nu + \sigma_l - l\sigma_3$ for a loop with l emerging helices [3, 4] where $\sigma_l = \epsilon l(2-l)/16 + \epsilon^2 l(l-2)(8l-21)/512 + \mathcal{O}(\epsilon^3)$ in an $\epsilon = 4-d$ expansion. One obtains $c_1 = 2.06$ for terminal loops present in hairpin structures and $c_2 = 2.14$ for internal loops.

The same analysis holds if one considers different topologies, namely peeling off one strand from the other starting from a nick. In this case one can show that $c = 0$ for an ideal polymer and $c = 0.092$ for a self avoiding polymer [3, 4].

Application of force to loops also alters the value of the loop exponent, which has been shown by Hanke et al. [5].

D. EFFECT OF PARAMETERS ON FEATURES OF THE FORCE-EXTENSION CURVE

Different parameters of the model are linked to certain features of the force extension curve. The chemical potentials g_i^0 determine the critical forces (fig. S1), the segment lengths l_i affect the maximal extensions (fig. S2) of each state and the off-diagonal V_{ij} determine the cooperativity of the transition (fig. S3).

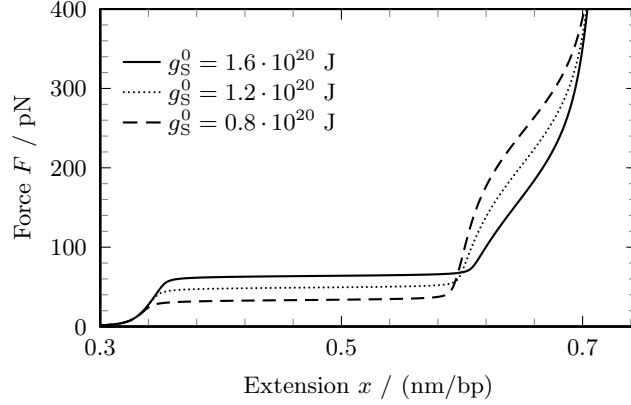


Figure S1: The chemical potentials g_i^0 influence the transition forces. The solid line shows the force extension curve for the parameters used in the main text for DNA without DDP. The dashed and the dotted line show stretching curves with different chemical potentials of the S-state g_S^0 while all other parameters are kept constant. Lowering g_S^0 leads to a decreasing plateau force of the BS-transition as the free energy difference between B- and S-states ($g_S(F) - g_B(F)$) decreases, see eq. (??) in the main text. At the same time the force of the SM-transition increases as the free energy difference between S- and M-states ($g_M(F) - g_S(F)$) increases.

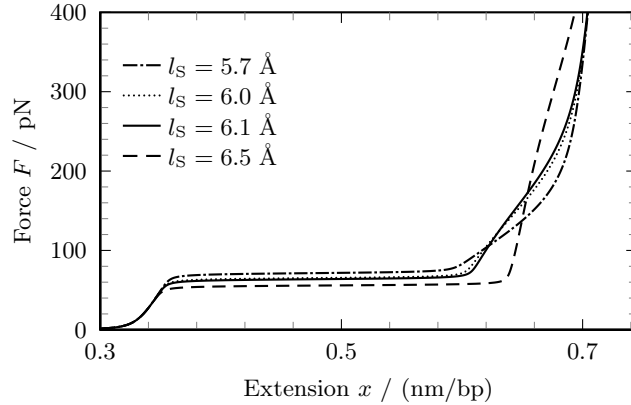


Figure S2: The segment lengths l_i determine the extensions between which the transitions occur. The solid line shows the force extension curve for the parameters used in the main text for DNA without DDP. The other curves have been obtained by by varying the segment length of the S-state l_S while keeping all other parameters constant. The effect of changing l_S is twofold. First, increasing l_S elongates the BS-plateau. As a side effect a larger l_S stabilizes the S-state as its $g_S^{\text{WLC}}(F)$ is lowered. This can also be concluded from eq. (S6). Thus, increasing l_S shifts the equilibrium towards the S-state, which is the same as decreasing g_S^0 , *cf.* fig. S1.

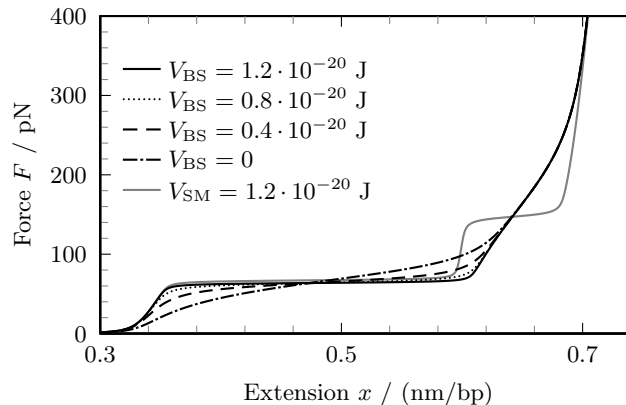


Figure S3: The interfacial energies V_{ij} determine the cooperativity of the transitions. The solid line shows the force extension curve for the parameters used in the main text for DNA without DDP. The other force extension curves have been obtained by varying V_{BS} or V_{SM} while keeping all other parameters constant. Lowering V_{BS} (dotted, dashed, and dash-dotted lines) smoothes the BS-transition and renders it less cooperative, which has been observed for DNA with DDP, *cf.* fig. ?? in the main text and the experiments by Krautbauer et al. [6]. V_{SM} has similar effects on the melting transition: Increasing V_{SM} from its original value 0 to $1.2 \cdot 10^{-20}$ J (gray curve) sharpens the denaturation transition.

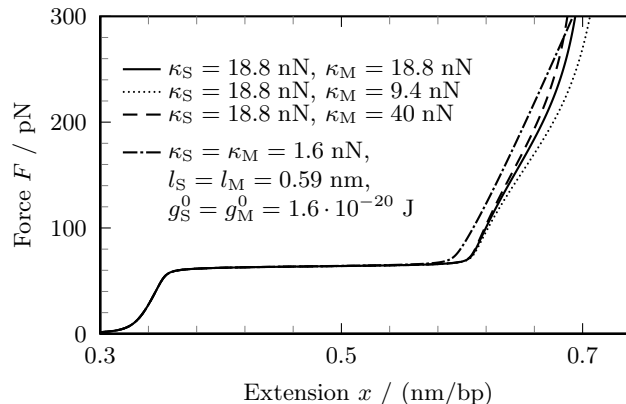


Figure S4: The influence of the stretch modulus on force extension curves is quite moderate. The solid line shows the force extension curve for the parameters used in the main text for DNA without DDP. The dashed and the dotted line show the data with $\kappa_M = 40$ nN and $\kappa_M = 9.4$ nN, respectively, while keeping all other parameters unchanged. One observes that changing κ_M by a factor 4 results in deviations of the extension by just a few percent even at extreme forces $F = 400$ pN. The dash-dotted line shows a force extension trace where $\kappa_S = \kappa_M = 1.6$ nN, and $l_S = l_M = 0.59$ nm have been used, which are the typical experimental values for two parallel ssDNA [7]. With this choice of parameters the force cannot discriminate between the S- and M-state anymore – the two states are degenerate. Therefore we have to set the chemical potentials equal, fit them again and obtain $g_S^0 = g_M^0 = 1.6 \cdot 10^{-20}$ J. Consequently the shoulder indicating a denaturation transition does not appear in the force extension curve in contrast to the other curves shown.

E. TABLES WITH MODEL PARAMETERS

Parameter	Symbol	λ -DNA	λ -DNA + DDP	Reference
segment length (nm)	l_B	0.34	0.34	Wenner et al. [8]
	l_S	0.61	0.60	fitted
	l_M	0.71	0.71	Hugel et al. [9]
persistence length (nm)	ξ_B	48	48	Wenner et al. [8]
	ξ_S	25	25	assumed
	ξ_M	3	3	Murphy et al. [10]
stretch modulus (nN)	κ_B	1.0	1.0	Wenner et al. [8]
	κ_S	2·9.4	2·9.4	Hugel et al. [9]
	κ_M	2·9.4	2·9.4	Hugel et al. [9]
chemical potential (10^{-20} J)	g_B^0	0.0	0.0	defined
	g_S^0	1.6	1.2	fitted
	g_M^0	2.4	2.8	fitted
interfacial energy (10^{-20} J)	V_{BB}, V_{SS}, V_{MM}	0.0	0.0	incorporated in g_i^0
	V_{BS}	1.2*	0.0	assumed, *disrupt stacked base pairs [11]
	V_{BM}	1.2*	0.0	assumed, *disrupt stacked base pairs [11]
	V_{SM}	0.0	0.0	

Table S1: Parameters for stretching curves at temperature $T = 293$ K.

Parameter	Symbol	λ -DNA	Reference
persistence length (nm)	$\xi_B(T)$	$48/(T/293 \text{ K})$	
	$\xi_S(T)$	$25/(T/293 \text{ K})$	
	$\xi_M(T)$	$3/(T/293 \text{ K})$	
chemical potential	$g_i^0(T) = h_i - Ts_i$		
enthalpy (10^{-20} J)	h_B	0.0	
	h_S	7.0	Clausen-Schaumann et al. [12], slightly rescaled
	h_M	15	fit for $c = 0$
	h_M	16	fit for $c = 3/2$
entropy (10^{-22} J/K)	s_B	0.0	
	s_S	1.8	Clausen-Schaumann et al. [12], slightly rescaled
	s_M	4.2	fit for $c = 0$
	s_M	4.6	fit for $c = 3/2$

Table S2: Temperature dependence of parameters for DNA without DDP. The enthalpy h_M and entropy s_M of the denatured state are determined by fixing the denaturation temperature T_c for zero force at $T_c = 348$ K.

-
- [1] J. F. Marko and E. D. Siggia, *Macromolecules* **28**, 8759 (1995).
[2] P.-G. de Gennes, *Scaling Concepts in Polymer Physics* (Cornell University Press, 1979).
[3] B. Duplantier, *Phys. Rev. Lett.* **57**, 941 (1986).
[4] Y. Kafri, D. Mukamel, and L. Peliti, *Phys. Rev. Lett.* **85**, 4988 (2000).
[5] A. Hanke, M. G. Ochoa, and R. Metzler, *Phys. Rev. Lett.* **100**, 018106 (2008).
[6] R. Krautbauer, H. Clausen-Schaumann, and H. E. Gaub, *Angew. Chem. Int. Edit.* **39**, 3912 (2000).
[7] S. B. Smith, Y. J. Cui, and C. Bustamante, *Science* **271**, 795 (1996).
[8] J. R. Wenner, M. C. Williams, I. Rouzina, and V. A. Bloomfield, *Biophys. J.* **82**, 3160 (2002).
[9] T. Hugel, M. Rief, M. Seitz, H. E. Gaub, and R. R. Netz, *Phys. Rev. Lett.* **94**, 048301 (2005).
[10] M. Murphy, I. Rasnik, W. Cheng, T. M. Lohman, and T. Ha, *Biophys. J.* **86**, 2530 (2004).
[11] J. SantaLucia, Jr., *Proc. Natl. Acad. Sci. U. S. A.* **95**, 1460 (1998).
[12] H. Clausen-Schaumann, M. Rief, C. Tolksdorf, and H. E. Gaub, *Biophys. J.* **78**, 1997 (2000).